1-1-2017

Interchangeable roles for E2F transcriptional repression by the retinoblastoma protein and $p27^{KIP1}$-cyclindependent kinase regulation in cell cycle control and tumor suppression

Michael J. Thwaites
Western University

Matthew J. Cecchini
Western University

Daniel T. Passos
Western University

Ian Welch
Western University

Frederick A. Dick
Western University, fdick@uwo.ca

AMERICAN SOCIETY FOR MICROBIOLOGY | Molecular and Cellular Biology®

RESEARCH ARTICLE

Interchangeable Roles for E2F Transcriptional Repression by the Retinoblastoma Protein and p27^{KIP1}–Cyclin-Dependent Kinase Regulation in Cell Cycle Control and Tumor Suppression

Michael J. Thwaites,[a,c] Matthew J. Cecchini,[a,c] Daniel T. Passos,[a,c] Ian Welch,[d] Frederick A. Dick[a,b,c]

London Regional Cancer Program,[a] Children's Health Research Institute,[b] Department of Biochemistry,[c] and Veterinary Services,[d] Western University, London, Ontario, Canada

ABSTRACT The mammalian G_1-S phase transition is controlled by the opposing forces of cyclin-dependent kinases (CDK) and the retinoblastoma protein (pRB). Here, we present evidence for systems-level control of cell cycle arrest by pRB-E2F and p27-CDK regulation. By introducing a point mutant allele of pRB that is defective for E2F repression (*Rb1*^{G}) into a p27^{KIP1} null background (*Cdkn1b*$^{-/-}$), both E2F transcriptional repression and CDK regulation are compromised. These double-mutant *Rb1*$^{G/G}$; *Cdkn1b*$^{-/-}$ mice are viable and phenocopy *Rb1*$^{+/-}$ mice in developing pituitary adenocarcinomas, even though neither single mutant strain is cancer prone. Combined loss of pRB-E2F transcriptional regulation and p27^{KIP1} leads to defective proliferative control in response to various types of DNA damage. In addition, *Rb1*$^{G/G}$; *Cdkn1b*$^{-/-}$ fibroblasts immortalize faster in culture and more frequently than either single mutant genotype. Importantly, the synthetic DNA damage arrest defect caused by *Rb1*$^{G/G}$; *Cdkn1b*$^{-/-}$ mutations is evident in the developing intermediate pituitary lobe where tumors ultimately arise. Our work identifies a unique relationship between pRB-E2F and p27-CDK control and offers *in vivo* evidence that pRB is capable of cell cycle control through E2F-independent effects.

KEYWORDS cell cycle, DNA damage, tumor suppressor, CDK, E2F, DNA damage checkpoints, cyclin-dependent kinases, tumor suppressor genes

Received 11 October 2016 **Accepted** 1 November 2016

Accepted manuscript posted online 7 November 2016

Citation Thwaites MJ, Cecchini MJ, Passos DT, Welch I, Dick FA. 2017. Interchangeable roles for E2F transcriptional repression by the retinoblastoma protein and p27^{KIP1}–cyclin-dependent kinase regulation in cell cycle control and tumor suppression. Mol Cell Biol 37:e00561-16. https://doi.org/10.1128/MCB.00561-16.

Address correspondence to Frederick A. Dick, fdick@uwo.ca.

Regulation of the cell cycle is critical to maintaining cellular homeostasis and to prevent the development of cancer (1). Mammalian cell division is primarily controlled at the G_1-S phase transition, and the moment of commitment is often described as the restriction point (2). Commitment to entering the cell cycle is controlled by two opposing forces, the retinoblastoma protein family (including pRB), which blocks entry, and cyclin-dependent kinases (CDKs), which drive advancement into S phase (3). The RB protein antagonizes S-phase entry by repressing E2F-regulated genes necessary for DNA replication (4). Working in opposition to pRB are CDKs (5), in particular cyclin D- and E-associated kinases, that phosphorylate and inactivate upstream regulators of cell cycle entry, including pRB and p27^{KIP1}, as well as stimulate the activation of downstream effectors of DNA replication (6, 7). While this suggests CDKs control pRB, a key target gene that is repressed by pRB-E2F is *CCNE1*, which encodes cyclin E, and this creates a regulatory loop whereby cyclin E/CDK2 becomes maximally active at almost the same time pRB is maximally phosphorylated and finally releases all E2Fs (4). In addition, CDK2's principal negative regulator, p27^{KIP1}, is phosphorylated and targeted

for degradation at virtually the same time (8). Due to this interplay between pRB and CDK activity, it has been difficult to place one upstream of the other in a regulatory pathway (4). Numerous studies suggest that either pRB-E2F or $p27^{KIP1}$-CDK2 interactions are essential for controlling quiescence or cell cycle entry commitment (9–17). For this reason, control of the G_1-S phase transition remains unclear. Furthermore, since much of the literature investigating G_1-S regulation focuses on regulatory events during cell cycle entry (4, 18), the roles for pRB-E2F and $p27^{KIP1}$-CDK interactions in cell cycle exit have been much less explored.

Cell cycle arrest by pRB has long been attributed to E2F regulation, because the minimal deletion mutant of pRB that is capable of binding E2Fs can block proliferation of Saos-2 cells (19, 20). These studies revealed a close correlation between pRB-E2F binding, transcriptional repression, and cell cycle arrest (20, 21). However, E2F binding mutants of pRB have a surprising retention of growth control activity in this assay (22–24), suggesting that other mechanisms contribute. Given that cell cycle control ultimately impinges on CDK regulation, a number of studies have connected pRB growth arrest activity in Saos-2 cells to CDK regulation through $p27^{KIP1}$ (25–27). First, E2F binding-deficient mutants of pRB induce $p27^{KIP1}$ expression in Saos-2 cell cycle arrest assays, and p27 expression is required for these mutants of pRB to induce arrest (27). Second, pRB stabilizes $p27^{KIP1}$ expression during induction of a G_1 arrest quite rapidly, and this precedes the decline in E2F-regulated targets by at least 24 h, suggesting CDK regulation occurs first (26). Moreover, Ji et al. also demonstrated that pRB is capable of binding and inhibiting the function of Skp2, the E3 ligase-targeting subunit responsible for polyubiquitination of p27 (26). Consistent with this, the increases in p27 levels seen following pRB expression in Saos-2 cells correlate with a decrease in Skp2 levels (25). Binne et al. showed that APC complexes containing Cdh1 are capable of using pRB as an adaptor for Skp2 binding and ubiquitination, thereby stimulating Skp2 degradation and promoting the stabilization of p27 (25). Collectively, these studies connect pRB regulation of the cell cycle to p27. However, the shortcoming of this work is its dependence on ectopic pRB expression, a physiological context in which pRB regulation of p27 genuinely contributes to proliferative control decisions has yet to emerge. A number of genetic crosses indicate that Skp2 loss can suppress pituitary tumorigenesis in $Rb1^{+/-}$ mice (28), even in combination with p53 deficiency (29). However, efforts to find p27-dependent growth arrest in tissues of these mice have been confounded by other cellular effects, such as apoptosis in the intermediate lobe of the pituitary (28). This has prevented the observation of proliferative control decisions in these cells that use a pRB-p27 axis. For this reason the pRB-p27 connection in proliferative control remains compelling, but its lack of detection in an endogenous scenario is a critical gap in our knowledge.

In order to study E2F-independent functions of pRB at an endogenous level, we developed a mutant mouse model in which pRB binding to E2Fs is disrupted by R461E and K542E mutations (called $Rb1^G$) (30). Importantly, the $Rb1^G$ mutant protein is expressed at wild-type (WT) levels and makes normal interactions with LXCXE motif-containing proteins (30). Surprisingly, we found that this mutation had little effect on control of cell proliferation, as $Rb1^{G/G}$ fibroblasts are capable of responding to serum starvation, p16 expression, DNA damage, and myogenic differentiation and in all cases show wild-type responses (30). In this study, we find that p27 expression is higher in $Rb1^{G/G}$ fibroblasts. In addition, double-mutant $Rb1^{G/G}$ and p27-deficient cells are defective for growth arrest in response to DNA damage in a manner that resembles $Rb1^{-/-}$ cells, including misregulation of CDK2 activity. Furthermore, while developmentally unremarkable, $Rb1^{G/G}$; $Cdkn1b^{-/-}$ mice display a highly penetrant tumor phenotype. Together our study demonstrates systems-level redundancy between pRB-E2F regulation and p27-CDK2 control, as the combined loss displays cell cycle defects that are absent from either mouse single mutant. In addition, this work provides proof of principle for transcription-independent coordination between the RB and the CDK pathways in endogenous growth control.

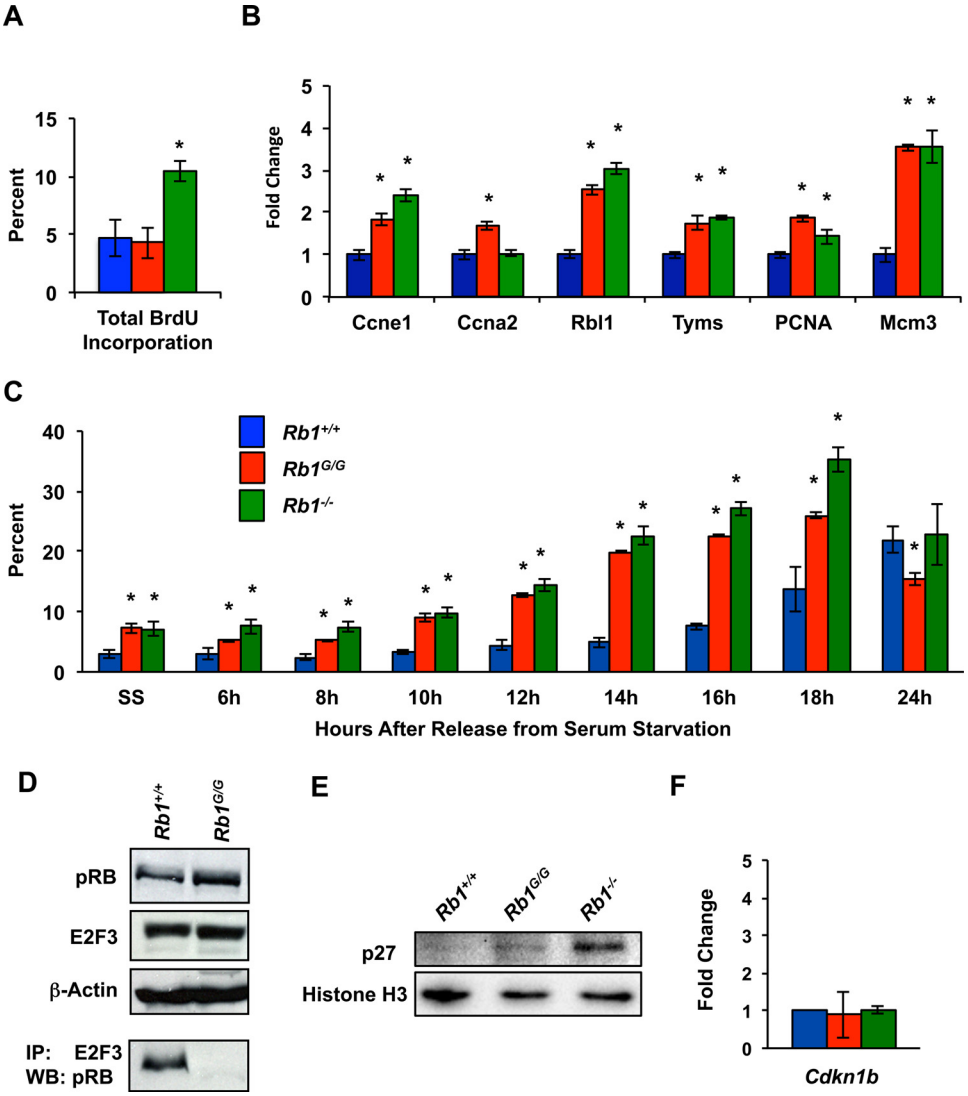

FIG 1 Increased expression of p27 in serum-starved *Rb1*$^{G/G}$ MEFs. (A) Fibroblast cells of the indicated genotypes were serum starved for 60 h and pulse-labeled with BrdU for 2 h, followed by staining for BrdU incorporation. The proportion of cells incorporating BrdU was determined by flow cytometry. (B) Fibroblasts were serum starved as described for panel A, and the relative mRNA levels of the indicated genes were determined. (C) Following serum starvation for 60 h, cells were restimulated to enter the cell cycle. Cultures were pulse-labeled with BrdU, harvested at the indicated time points, and analyzed by flow cytometry. (D) Whole-cell extracts were prepared from serum-starved (SS) wild-type and *Rb1*$^{G/G}$ MEFs. Western blot (WB) analyses were performed to assess relative expression of pRB and E2F3. Anti-E2F3 immunoprecipitations were blotted for pRB. (E) Immunoblotting of nuclear extracts isolated from serum-deprived MEFs using antibodies raised against p27 and histone H3. (F) Real-time quantitative PCR using primers to detect *Cdkn1b*. Values are presented relative to GAPDH. All error bars represent one standard deviation from the mean. An asterisk indicates a significant difference from the wild-type control using a *t* test ($P < 0.05$).

RESULTS

Posttranslational stabilization of p27 in *Rb1*$^{G/G}$ fibroblasts during quiescence. Our previously published analysis of *Rb1*$^{G/G}$ primary fibroblasts and mice indicates that loss of pRB-E2F repression fails to bypass cell cycle exit signals (30). Figure 1 shows an example of a serum starvation arrest in which wild-type, *Rb1*$^{G/G}$, and knockout cells were serum starved for 60 h. Under these culture conditions, wild-type and *Rb1*$^{G/G}$ cells reduce bromodeoxyuridine (BrdU) incorporation equivalently, while *Rb1*$^{-/-}$ cells are defective (Fig. 1A). However, analysis of mRNA levels of common E2F target genes shows that *Rb1*$^{G/G}$ displays a defect in repression similar to that of *Rb1*$^{-/-}$ (Fig. 1B). Importantly, while cell cycle exit is normal in this scenario, pRB's well-studied role for

restraining E2F activation during cell cycle entry following serum stimulation is compromised in *Rb1*$^{G/G}$ cells, and they enter the cell cycle with kinetics similar to those of knockout controls (Fig. 1C). Consistent with these findings, the R461E and K542E mutations encoded by the *Rb1*^{G} allele prevent stable interactions with E2Fs. We used immunoprecipitation (IP) and Western blot assays to evaluate pRB-E2F3 interactions in serum-starved cells, and these reveal a robust defect (Fig. 1D) (30). Since *Rb1*$^{G/G}$ cells are functional for cell cycle arrest in assays where *Rb1*$^{-/-}$ cells are not (30), we searched for growth control mechanisms parallel to pRB-E2F repression that are pRB dependent. Building on previous findings of p27 stabilization in cancer cells and *Rb1*$^{-/-}$ mouse embryonic fibroblasts (MEFs), we sought to determine if this same effect was seen in our mutant *Rb1*$^{G/G}$ cells. Following serum deprivation of asynchronously proliferating cultures, *Rb1*$^{G/G}$ MEFs demonstrated a modest increase in p27 protein levels coincident with G_1 arrest (Fig. 1E). Importantly, p27 mRNA levels quantitated by quantitative reverse transcription-PCR (qRT-PCR) remain the same as those of wild-type cells during serum deprivation, indicating that the change observed is likely due to a posttranslational effect (Fig. 1F). This finding is consistent with the posttranslational stabilization of p27 observed in Saos-2 cells induced to arrest following expression of E2F binding-deficient mutants of pRB (27). The increased p27 in response to loss of E2F regulation may be related to the ability of *Rb1*$^{G/G}$ MEFs to maintain proliferative control despite defective E2F binding.

***Rb1*$^{G/G}$; *Cdkn1b*$^{-/-}$ mice are highly cancer prone.** To determine if p27 expression in *Rb1*$^{G/G}$ cells is responsible for the maintenance of cell cycle control, we crossed *Rb1*$^{G/G}$ mice with p27-deficient (*Cdkn1b*$^{-/-}$) animals. Compound mutant mice display viability at weaning similar to that of the *Rb1*$^{G/G}$ genotype alone and without obvious anatomical defects, suggesting the combination of *Rb1*$^{G/G}$ and *Cdkn1b*$^{-/-}$ deficiency is no different than either single mutant alone (Fig. 2A and Table 1) (30). While double-mutant *Rb1*$^{G/G}$; *Cdkn1b*$^{-/-}$ mice show normal development, we aged cohorts of double- and single-mutant mice and discovered that *Rb1*$^{G/G}$; *Cdkn1b*$^{-/-}$ mice succumb to pituitary tumors with an average tumor-free survival of 214 days (Fig. 2B). Necropsies of these mice revealed pituitary tumor masses characteristic of *Rb1*-deficient animals (Fig. 2C). By comparison, neither *Rb1*$^{G/G}$ nor *Cdkn1b*$^{-/-}$ mice displayed cancer susceptibility (Fig. 2B and C), and this is consistent with prior reports of mixed 129/B6 *Cdkn1b*$^{-/-}$ mice (31). Interestingly, *Rb1*$^{G/+}$; *Cdkn1b*$^{-/-}$ mice also succumb to pituitary tumor formation with a delayed latency compared to double mutants and with approximately 75% penetrance (Fig. 2B and C). PCR genotype analysis revealed that loss of the wild-type copy of *Rb1* is ubiquitous in these tumors (Fig. 2D). The *Rb1*$^{G/+}$; *Cdkn1b*$^{-/-}$ tumor phenotype is highly reminiscent of *Rb1*$^{+/-}$; *Cdkn1b*$^{-/-}$ tumors in terms of latency and the requirement for loss of heterozygosity of *Rb1* (31). Based on this observation, the *Rb1*^{G} allele appears to be the functional equivalent of an *Rb1* null allele when combined with p27 deficiency in this context. These genetic data also imply that p27 function is required for pRB-dependent tumor suppression when pRB is defective for E2F binding, and that pRB-E2F control is critical in the absence of p27.

Compound mutant *Rb1*$^{G/G}$; *Cdkn1b*$^{-/-}$ MEFs enter quiescence following serum deprivation. The normal development of double-mutant animals suggests that pRB-mediated repression of E2Fs, as well as deficiency for p27, are dispensable for a variety of cell cycle exit decisions that occur as part of a normal mammalian developmental program. However, emergence of pituitary adenocarcinomas indicates that this combination is important in some contexts for the mitigation of tumorigenesis. We therefore sought to understand if specific cell cycle control functions are lost in *Rb1*$^{G/G}$; *Cdkn1b*$^{-/-}$ cells. Since both pRB and p27 are implicated in quiescence, we assessed their separate and combined contributions to serum deprivation-induced arrest (2). Asynchronously proliferating cultures of primary fibroblasts for each of the wild-type, *Rb1*$^{G/G}$, *Cdkn1b*$^{-/-}$, double-mutant *Rb1*$^{G/G}$; *Cdkn1b*$^{-/-}$, and *Rb1*$^{-/-}$ mice were analyzed for their proliferative state by BrdU labeling and flow cytometry. Figure 3A shows baseline levels of BrdU incorporation for each genotype while actively proliferating, and

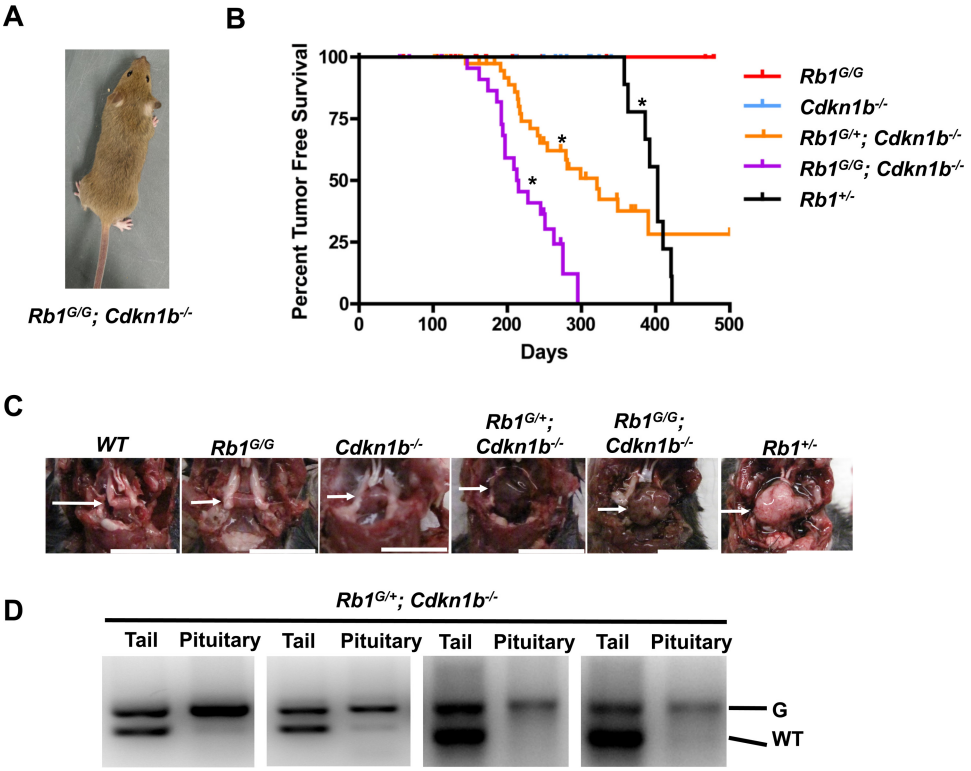

FIG 2 Cancer susceptibility in *Rb1*$^{G/G}$; *Cdkn1b*$^{-/-}$ mice. (A) Picture of young adult double-mutant *Rb1*$^{G/G}$; *Cdkn1b*$^{-/-}$ mouse. (B) Kaplan-Meyer analysis of tumor-free survival for mice of the indicated genotypes. Mice were monitored until natural endpoint, and those having tumors are shown. *Rb1*$^{G/G}$; *Cdkn1b*$^{-/-}$, *Rb1*$^{G/+}$; *Cdkn1b*$^{-/-}$, and *Rb*$^{+/-}$ mice are significantly different from one another and from all single-mutant controls using the log rank test ($P < 0.05$). (C) Macroscopic images of pituitaries of mice from the indicated genotypes at necropsy. Scale bars are 1 cm. (D) Genotyping of tumor and tail DNA isolated from *Rb1*$^{G/+}$; *Cdkn1b*$^{-/-}$ (G) mice demonstrating loss of heterozygosity in the tumor tissue.

it shows *Rb1*$^{G/G}$; *Cdkn1b*$^{-/-}$ and *Rb1*$^{-/-}$ have statistically elevated BrdU incorporation levels. Cells were subsequently washed and transferred to 0.1% serum to induce arrest for 60 h before pulse-labeling with BrdU. While asynchronously cycling, double-mutant *Rb1*$^{G/G}$; *Cdkn1b*$^{-/-}$ MEFs exhibit an increase of cells in S phase while proliferating, and these cells were able to restrict S-phase entry following serum deprivation to a level equivalent to that of wild-type fibroblasts (Fig. 3B). Importantly, the incomplete response in *Rb1*$^{-/-}$ cells indicates that this is a pRB-dependent process that *Rb1*$^{G/G}$; *Cdkn1b*$^{-/-}$ cells are capable of executing. Similarly, analysis of CDK2 activity by

TABLE 1 *Rb1*$^{G/G}$; *Cdkn1b*$^{-/-}$ mice are produced at ratios similar to those of *Rb1*$^{G/G}$ mice[a]

Genotype	No. of live animals observed[b] (expected)
Rb1$^{+/+}$; *Cdkn1b*$^{+/+}$	25 (15)
Rb1$^{+/+}$; *Cdkn1b*$^{+/-}$	27 (29)
Rb1$^{+/+}$; *Cdkn1b*$^{-/-}$	12 (15)
Rb1$^{G/+}$; *Cdkn1b*$^{+/+}$	40 (29)
Rb1$^{G/+}$; *Cdkn1b*$^{+/-}$	72 (59)
Rb1$^{G/+}$; *Cdkn1b*$^{-/-}$	22 (29)
Rb1$^{G/G}$; *Cdkn1b*$^{+/+}$	11 (15)
Rb1$^{G/G}$; *Cdkn1b*$^{+/-}$	19 (30)
Rb1$^{G/G}$; *Cdkn1b*$^{-/-}$	8 (15)
Total	236

[a]Compound heterozygous mice were crossed (*Rb1*$^{G/+}$; *Cdkn1b*$^{+/-}$ × *Rb1*$^{G/+}$; *Cdkn1b*$^{+/-}$), and the resulting progeny were genotyped.
[b]The number of live animals obtained at 2 weeks is shown for each genotype, and the expected number based on Mendelian inheritance is displayed in parentheses.

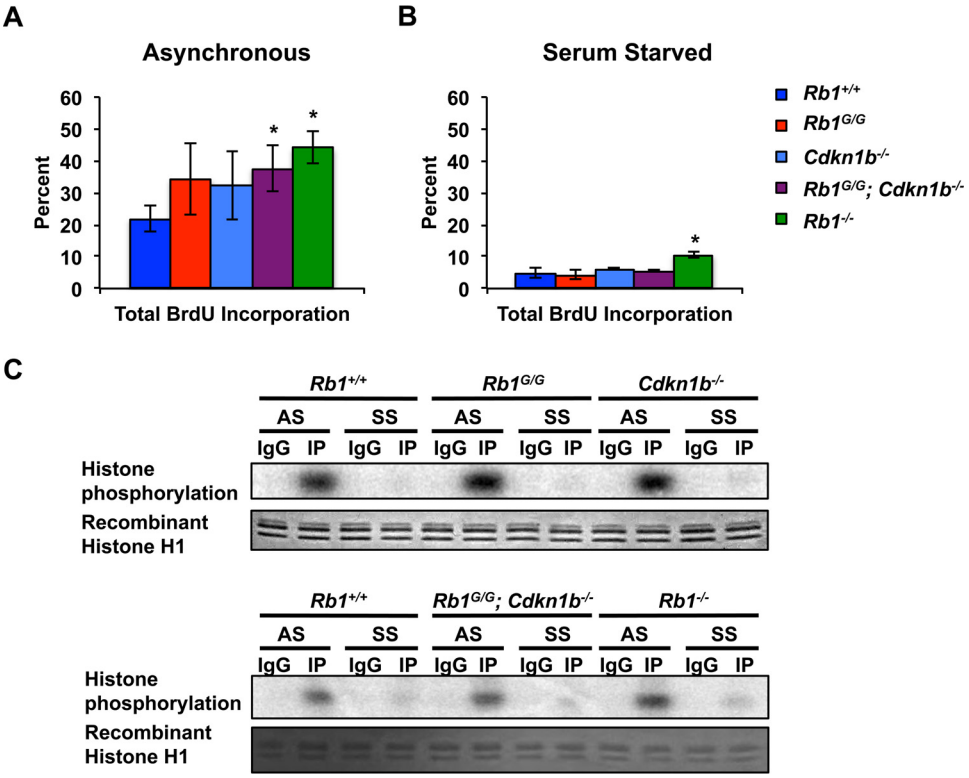

FIG 3 Compound mutant *Rb1*$^{G/G}$; *Cdkn1b*$^{-/-}$ MEFs enter quiescence. (A) Asynchronously growing MEFs were pulsed-labeled with BrdU for 2 h, followed by staining for BrdU incorporation and analysis by flow cytometry. (B) Proliferating cells were serum deprived for 60 h and pulse-labeled with BrdU for 2 h, followed by staining for BrdU incorporation and flow cytometry. All error bars represent one standard deviation from the mean. An asterisk indicates a significant difference from the wild-type control using a *t* test ($P < 0.05$). (C) CDK2 kinase activity was determined by incubation of immunoprecipitated CDK2 complexes isolated from the indicated genotypes of cells under asynchronous growth conditions (AS) or serum-starved conditions (SS). Proteins isolated by immunoprecipitation with anti-CDK2 antibodies (IP) or the control (IgG) were mixed with recombinant histone H1 and [γ-^{32}P]ATP, incubated, and resolved by gel electrophoresis and exposed to a phosphosensitive plate. Coomassie staining of the recombinant histone H1 serves as a loading control.

IP-kinase assays reveals that single-mutant *Rb1*$^{G/G}$ and *Cdkn1b*$^{-/-}$ cells were also capable of inhibiting CDK2 kinase activity (Fig. 3C), as were double-mutant *Rb1*$^{G/G}$; *Cdkn1b*$^{-/-}$ MEFs. Some residual CDK2 activity was also observed in the *Rb1*$^{-/-}$ cells following serum deprivation, reflecting the defect in G_1 arrest observed in *Rb1*$^{-/-}$ MEFs (Fig. 3C). Maintenance of quiescence and CDK2 inhibition in double-mutant *Rb1*$^{G/G}$; *Cdkn1b*$^{-/-}$ MEFs agrees with the developmental milestones observed in *Rb1*$^{G/G}$; *Cdkn1b*$^{-/-}$ mice, as quiescence induction is a component of normal development (32).

Compound mutant *Rb1*$^{G/G}$; *Cdkn1b*$^{-/-}$ cells display defective cell cycle control in response to DNA damage. The detection of malignancies later in life in *Rb1*$^{G/G}$; *Cdkn1b*$^{-/-}$ mice likely indicates that additional mutations occur prior to tumorigenesis. Therefore, we next looked at the ability of single- and double-mutant *Rb1*$^{G/G}$; *Cdkn1b*$^{-/-}$ MEFs to arrest the cell cycle in response to DNA damage, as a defect in this response could facilitate the acquisition of new mutations. We subjected asynchronously proliferating cells to three different DNA-damaging agents, gamma irradiation (IR), cisplatin, and hydrogen peroxide, and pulse-labeled cells with BrdU 48 h later. The percentage of BrdU-positive cells was then determined by flow cytometry (Fig. 4A). With each treatment, double-mutant *Rb1*$^{G/G}$; *Cdkn1b*$^{-/-}$ and *Rb1*$^{-/-}$ cells failed to block BrdU incorporation. Interestingly, some single mutants showed modest defects in their response to cisplatin and hydrogen peroxide (Fig. 4A). However, analysis of DNA content by propidium iodide staining following IR showed that both double-mutant *Rb1*$^{G/G}$; *Cdkn1b*$^{-/-}$ and *Rb1*$^{-/-}$ MEFs exhibit a high proportion of cells with 8N DNA content, implying a strong defect in the regulation of DNA replication following

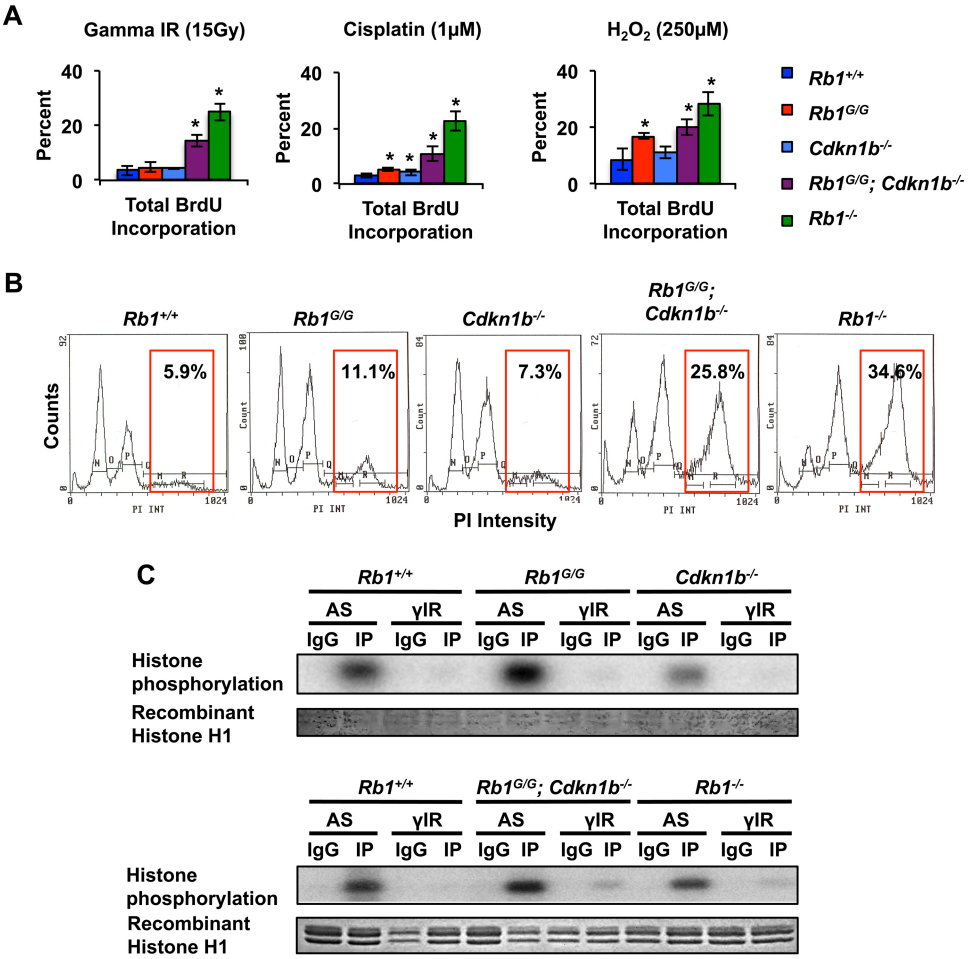

FIG 4 Mutant *Rb1*$^{G/G}$; *Cdkn1b*$^{-/-}$ MEFs display defective cell cycle control in response to DNA damage. (A) MEFs were treated with the indicated dose of DNA damaging agents. Forty-eight hours later, cells were pulsed with BrdU, stained, and analyzed by flow cytometry. All error bars represent one standard deviation from the mean. An asterisk indicates a significant difference from the wild-type control using a *t* test ($P < 0.05$). (B) Propidium iodide (PI) staining of MEFs treated with 15 Gy of ionization radiation showing DNA content of cells. Red boxes outline an area of >4N DNA content, with the number representing the percentage of cells in that box. (C) Kinase assays were performed using CDK2 kinases isolated from asynchronously growing (AS) cells or following treatment with ionizing radiation (γIR). Kinase activity was determined by incubation of immunoprecipitated CDK2 complexes with recombinant histone H1 and with [γ-^{32}P]ATP, followed by gel electrophoresis and exposure to a phosphosensitive plate. Coomassie staining of recombinant histone H1 served as a loading control.

damage (Fig. 4B). This suggests that loss of both pRB-E2F binding and p27 together results in a defective DNA damage checkpoint, leading to endoreduplication in a manner that is very similar to complete *Rb1* deficiency. We also tested CDK2 activity from extracts of IR-treated cells using an IP-kinase assay. Once again, *Rb1*$^{G/G}$ and *Cdkn1b*$^{-/-}$ single-mutant MEFs were able to reduce CDK2 kinase activity down to background levels, whereas double-mutant *Rb1*$^{G/G}$; *Cdkn1b*$^{-/-}$ and *Rb1*$^{-/-}$ MEFs were only able to partially restrict CDK2 kinase activity, mirroring the result seen by BrdU incorporation analysis (Fig. 4C). The failure of double-mutant *Rb1*$^{G/G}$; *Cdkn1b*$^{-/-}$ MEFs to arrest in response to DNA damage provides a possible framework to explain the eventual development of pituitary adenocarcinomas in older mice. Therefore, in the context of DNA damage, *Rb1*$^{G/G}$; *Cdkn1b*$^{-/-}$ animals may be unable to respond appropriately to the insult, allowing for the development of further mutations and the clonal expansion of tumorigenic cells.

Compound mutant *Rb1*$^{G/G}$; *Cdkn1b*$^{-/-}$ fibroblasts undergo rapid immortalization in culture. We also modeled the acquisition of cancer-enabling mutations over time using a 3T3 immortalization assay to assess the different *Rb1* and *Cdkn1b* mutant

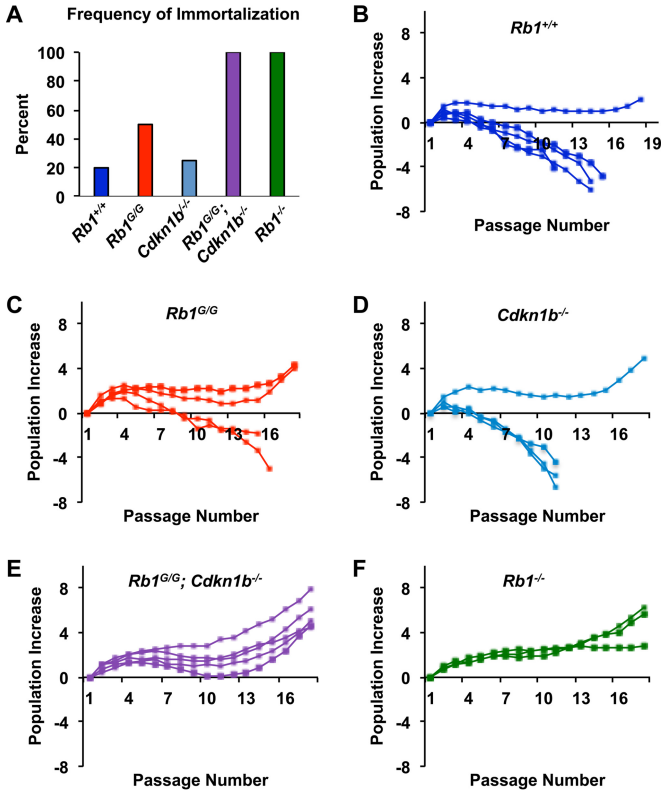

FIG 5 *Rb1*$^{G/G}$; *Cdkn1b*$^{-/-}$ MEFs undergo rapid immortalization in response to oxidative stress. (A) Percentage of cultures that immortalized within 20 passages of 3T3 culture. Immortalization was defined as continued positive population growth following a decline in cell number at intermediate passages. (B to F) Population growth of MEFs of the indicated genotypes was plotted against passage number. Cells were plated at a density of 1×10^6 cells per 10-cm plate, and they were reseeded at the same density every 3 days. Population increase was calculated according to the formula $\log_{10}$ (recovered/seeded)/$\log_{10}$ 2 and plotted cumulatively over 20 passages or until no viable cells were left in the culture.

genotypes. By passaging primary MEFs in a 3T3 protocol, we were able to subject them to long-term oxidative stress (33) and its resultant DNA damage (33) and determined genotype-specific responses. We categorized entry into senescence in this assay as the first passage that displays a negative population increase. Furthermore, we categorized immortalization as the first passage where positive population increases resumed and continued uninterrupted for the remainder of the 20-passage experiment. From this analysis we note that all attempts to immortalize *Rb1*$^{G/G}$; *Cdkn1b*$^{-/-}$ and *Rb1*$^{-/-}$ MEFs were successful (Fig. 5A), whereas at least half of the single mutants or wild-type controls entered senescence and never resumed proliferation. All wild-type, single-mutant, and *Rb1*$^{G/G}$; *Cdkn1b*$^{-/-}$ double-mutant cells entered senescence, as evidenced by negative growth trends (Fig. 5B to F). In this assay, only *Rb1*$^{-/-}$ cells spontaneously immortalized without entering senescence (Fig. 5F). Notably, double-mutant *Rb1*$^{G/G}$; *Cdkn1b*$^{-/-}$ cells demonstrated a longer period of positive growth than single mutants (Fig. 5E), and they spent fewer passages in senescence before resuming continual expansion. A similar profile of brief arrest before rapid expansion was exhibited by most *Rb1*$^{-/-}$ cell cultures (Fig. 5F), and this further emphasizes the similarity between the *Rb1*$^{G/G}$; *Cdkn1b*$^{-/-}$ and *Rb1*$^{-/-}$ genotypes in this assay. This result demonstrates that cells containing mutations to abolish pRB-E2F repression and loss of p27 are poised to immortalize, and this property is consistent with their inability to arrest the cell cycle following DNA damage.

Compound mutant *Rb1*$^{G/G}$; *Cdkn1b*$^{-/-}$ cells in the embryonic intermediate pituitary demonstrate radioresistant DNA synthesis. Given the propensity of *Rb1*$^{G/G}$; *Cdkn1b*$^{-/-}$ mice to develop pituitary tumors, as demonstrated in this report, and the

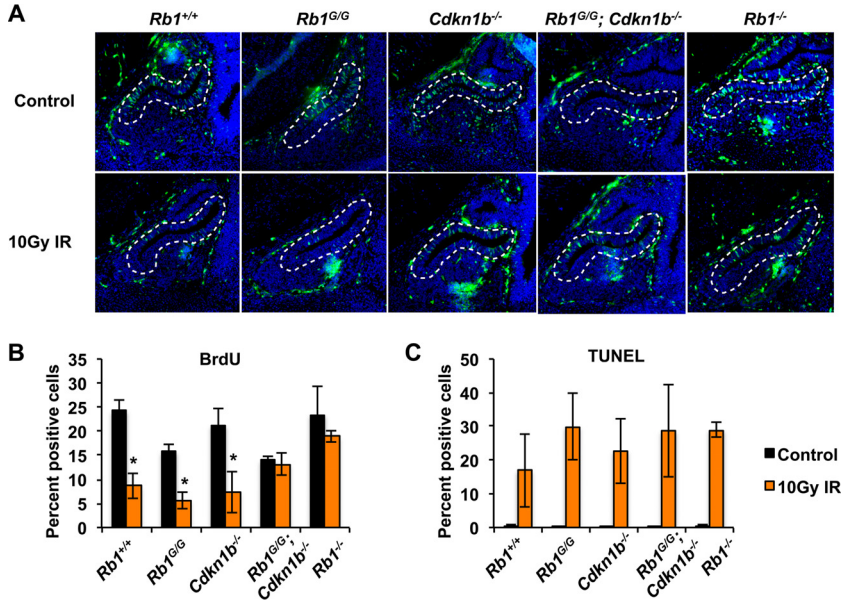

FIG 6 Double-mutant *Rb1*$^{G/G}$; *Cdkn1b*$^{-/-}$ embryonic pituitaries exhibit radioresistant DNA synthesis. (A) Representative images of E13.5 pituitaries stained for BrdU from control or irradiated embryos. The intermediate lobe of the pituitary is outlined in dashed lines. (B) The percentage of BrdU-positive cells in the intermediate lobe of the pituitary was determined from the indicated genotypes of mice from control or irradiated groups. All error bars represent one standard deviation from the means. An asterisk indicates a significant difference from the wild-type control using a *t* test ($P < 0.05$). (C) Tissue sections were stained with TUNEL, and positive cells within the intermediate lobe of the pituitary were quantitated for in the indicated genotypes either with or without irradiation. All error bars represent one standard deviation from the mean, and there are no significant differences among the treated groups.

long history of *Rb1* null alleles to predispose mice to this tumor type, we sought to assess cell cycle regulation in this tissue. As the intermediate lobe of the pituitary gland gives rise to the adenocarcinomas previously reported in *Rb1* mutant mice (34, 35), we chose to investigate the DNA damage response specifically in these cells. In order to analyze acute response to DNA damage in the pituitary, embryos at 13.5 days of gestation (E13.5) were used, as the peak proliferation of the pituitary occurs at this time and postnatal proliferation is largely undetectable (36). Pregnant mothers were exposed to a dose of 10 Gy of ionizing radiation 4 h prior to injection with BrdU and sacrificed 2 h later. Tissue sections of embryos were cut to expose the developing pituitary, and sections were stained to detect BrdU (Fig. 6A). Wild-type as well as single-mutant *Rb1*$^{G/G}$ and *Cdkn1b*$^{-/-}$ embryos displayed a robust reduction in BrdU incorporation following DNA damage, as determined by counting BrdU-positive nuclei in the intermediate lobe of the pituitary (Fig. 6B). Similar to our findings in cell culture, both *Rb1*$^{G/G}$; *Cdkn1b*$^{-/-}$ and *Rb1*$^{-/-}$ embryos failed to display a significant reduction of BrdU incorporation following irradiation (Fig. 6B). Terminal deoxynucleotidyltransferase-mediated dUTP-biotin nick end labeling (TUNEL) staining of parallel sections was performed to quantitate double-stranded DNA breaks and revealed similar levels of damage among all genotypes (Fig. 6C). This outcome indicates that the cell cycle arrest defect following DNA damage in double-mutant *Rb1*$^{G/G}$; *Cdkn1b*$^{-/-}$ cells is evident in both cell culture and *in vivo* settings, and it occurs in the cell population that eventually gives rise to the tumor phenotype seen in these mice. Thus, the regulation of E2Fs by pRB as well as the CDK control via p27 are each individually dispensable for cell cycle control, and simultaneous loss of both leads to an insensitivity to DNA damage signaling and a predisposition to cancer.

DISCUSSION

Our findings support the existence of a link between pRB-mediated growth control and CDK regulation that is independent of pRB-E2F control of transcription. The similar

defect in DNA damage-induced growth arrest between *Rb1*$^{G/G}$; *Cdkn1b*$^{-/-}$ and *Rb1*$^{-/-}$ cells implies that E2F-independent growth control by pRB is dependent on CDK regulation by p27. In addition, we find that defective E2F binding by pRB or loss of p27 is individually tolerated in most arrest assays, suggesting their functions are somewhat interchangeable. Lastly, cancer incidence and latency of our *Rb1*$^{G/+}$; *Cdkn1b*$^{-/-}$ mice are very similar to those of previously published *Rb1*$^{+/-}$; *Cdkn1b*$^{-/-}$ mice (31), and this suggests that in the absence of p27, the *Rb1*^{G} allele is approximately equivalent to an *Rb1* null. Collectively, these data point to a strong interdependence of CDK and E2F regulation.

Previous studies of endogenous pRB function in mice have typically relied on knockout alleles. This approach to mechanistic understanding is constrained by several limitations that are overcome in our targeted knock-in approach. First, other pRB family members, p107 and p130, increase in expression in pRB's absence (3, 37). Additionally, pRB is reported to interact with over 100 proteins (38), so complete loss of pRB disrupts all of these binding partners, obscuring the roles of individual interactions. For these reasons, our *Rb1*$^{G/G}$ model specifically mitigates these problems, allowing us to demonstrate a role for pRb-E2F interactions *in vivo* in tumor suppression. Surprisingly, these studies and our previous report of these mice reveal that loss of pRB-E2F transcriptional repression functions in parallel with p27 in growth control and tumor suppression (30).

We have found that disruption of pRB-E2F interactions acts synergistically with p27 deletion to bring about a loss of cell cycle control. The degree of disruption is similar to complete pRB knockout, and this implies that p27 lies downstream of pRB in an E2F-independent growth arrest pathway. A number of previous reports have identified a link between pRB and p27 as a means of cross talk between the RB pathway and the CDK regulatory pathway (25, 26). pRB has been shown to interact with Skp2 as well as the APC^{Cdh1} complex (25, 26). These interactions allow pRB to reduce available Skp2 either through facilitation of Skp2 ubiquitination by APC^{Cdh1} or through Skp2 sequestration. Ultimately, these interactions stabilize p27 expression and block CDK activity independent of pRB-E2F transcriptional repression. However, each of these reports relies on overexpression of pRB as the growth-arresting stimulus, leaving in question the physiological circumstances where this mechanism works. We think this report offers proof of principle for a pRB-p27 regulatory axis; in addition to showing that it functions in DNA damage-induced arrest, its inactivation renders mice cancer prone. This argues that the pRB-p27 connection is critical to what makes pRB a tumor suppressor.

The interplay between pRB and p27 identified in this study may also provide important insights into the utilization of targeted therapies aiming to restore cell cycle control. A number of CDK4/6 inhibitors have been developed in attempts to reestablish the G_1 checkpoint in cancer cells (39–41). Since CDK4/6 inhibition is known to arrest proliferation only when pRB is functional, these inhibitors are generally given to patients with pRB-positive cancers. However, pRB status alone does not indicate the effectiveness of these treatments (42). Our analysis of G_1 checkpoint control may provide some insight into ways to maximize the effectiveness of these treatments. We suggest that reactivation of the pRB pathway by CDK4/6 inhibitors is more effective in cancers with inherently high p27 expression or whose p27 stabilization pathways remain active.

Overall, our findings reveal a role for pRB in DNA damage-induced cell cycle arrest beyond repression of E2F transcriptional activity that utilizes p27 and CDK inhibition. Furthermore, our work suggests a functional context for the regulation of p27 by pRB that has been elusive.

MATERIALS AND METHODS

Cell culture methods. Mouse embryonic fibroblasts (MEFs) were derived from E13.5 embryos of the indicated genotypes. Asynchronous cells were cultured using standard methods in Dulbecco's modified Eagle's medium containing 10% fetal bovine serum (FBS), 2 mM L-glutamine, 50 U/ml penicillin, and 50 μg/ml streptomycin. Cells subjected to serum deprivation were cultured in the above-described medium, except it only contained 0.1% FBS.

DNA damage induction. MEFs subjected to gamma irradiation were plated at low density at passage 4. The next day, medium was changed prior to exposure to a cobalt 60 source until a dose of 15 Gy was received. Medium was changed again the next morning, and cells were harvested 48 h after treatment. Cells treated with DNA-damaging agents cisplatin and H_2O_2 were plated at low density at passage 4 and then the next day were switched to medium containing the indicated drug at a concentration of 1 μM for cisplatin and 250 μM for H_2O_2. Cells were incubated in the drug containing medium for 48 h before harvest for downstream applications.

Cell cycle analysis. Cells were pulsed with BrdU under different growth conditions: asynchronous culture, serum deprived, serum stimulated, or various sources of DNA damage for a duration of 2 h. Cell cycle analysis was then carried out by following previously published protocols (43).

mRNA quantitation. RNA isolation was carried out using TRIzol reagent according to the manufacturers' instructions and previously published protocols (30). mRNA levels of p27 were analyzed by qRT-PCR using iQ Sybr green supermix (Bio-Rad) and the following primers against p27 and glyceraldehyde-3-phosphate dehydrogenase (GAPDH): p27 Fwd (5′AGATACGAGTGGCAGGAGGT 3′), p27 Rev (5′ ATGCC GGTCCTCAGAGTTTG 3′), GAPDH Fwd (5′ GCACAGTCAAGGCCGAGAAT 3′), and GAPDH Fwd. (5′ GCCTT CTCCATGGTGGTGAA 3′). Expression levels of common E2F target genes *Pcna1*, *Ccne1*, *Ccna2*, *Tyms*, *Rbl1*, and *Mcm3* were determined using the Quantigene Plex 2.0 reagent system from Affymetrix as previously described (44). Expression levels were normalized to actin.

3T3 assay. Passage 3 MEFs were plated at a density of 1×10^6 cells per 10-cm culture dish in Dulbecco's modified Eagle's medium containing 10% calf serum, 2 mM L-glutamine, 50 U/ml penicillin, and 50 μg/ml streptomycin. Three days after plating, cells were counted and replated at the same density, 1×10^6 cells per 10-cm dish. This procedure was repeated until passage 20. Population increase was calculated according to the following formula: $\log_{10}$ (recovered/seeded)/$\log_{10}$ 2. Cells were considered successfully immortalized if the population growth was positive at the end of the 20 passages.

Protein interaction analysis and Western blotting. Nuclear extracts were prepared from MEFs, and Western blotting was carried out using previously described protocols (30). Antibodies raised against p27 (C-19; sc-528) and histone H3 (ab70550) were used for Western blotting. pRB-containing complexes were immunoprecipitated from whole-cell extracts using anti-E2F3 C-18 (Santa Cruz) bound to G-Sepharose beads (GE Healthcare). IPs were rocked for 1 h at 4°C and then washed twice with IP wash buffer (10 mM Tris, pH 7.5, 200 mM NaCl, 1.5 mM $MgCl_2$, 2 mM EDTA, 0.1% NP-40) and boiled in SDS-PAGE sample buffer. Samples were Western blotted using standard techniques. E2F3 was detected by PG37 (Upstate), pRB was detected by G3-245 (BD Pharmingen), and actin was detected with monoclonal antibody AC-74 (Sigma).

Phenotypic analysis of animals. *Cdkn1b*$^{-/-}$ mice (B6.129S4-Cdkn1b^{tm1Mlf}/J) have been described previously and were obtained from the Jackson Laboratory and genotyped as recommended (45). *Rb1*$^{G/G}$ mice were genotyped as previously described (30). All animals were housed and handled as approved by the Canadian Council on Animal Care. Mice were monitored for tumor development. Mice were sacrificed at natural endpoint. Survival data were subjected to Kaplan-Meier analysis, and significant differences were compared using a log rank test. For DNA damage experiments, pregnant mothers at day 13.5 of gestation were subjected to 10 Gy IR followed by a 2-h pulse of BrdU 4 h after IR treatment.

Histology and microscopy. E13.5 embryos treated with 10 Gy of IR were removed from the uterus and fixed whole in phosphate-buffered saline (PBS) containing 4% paraformaldehyde (PFA) for 24 h. They were next placed in PBS containing 30% sucrose to dehydrate the samples for a minimum of 3 days. Embryos were then dried and mounted in Cryomatrix (6769006; Thermo Scientific), frozen using liquid nitrogen, and stored at −80°C (46). Sagittal pituitary sections were cut using a Leica cryostat (CM 3050S) in 8-μm sections and mounted on slides which were stored at −80°C. Slides were acclimated to room temperature prior to staining.

For BrdU staining, slides were rehydrated in PBS and inserted into a Shandon Sequenza cassette holder (73310017; Thermo Scientific). Five hundred microliters of 2N HCl was added to the slides and incubated for 20 min at room temperature. Slides were washed twice with 0.1 M $Na_2B_4O_7$, pH 8.5, for 5 min per wash. Slides were then put into a Coplin jar containing 10 mM sodium citrate, pH 6, and microwaved for 10 min on a low power level, followed by a 20-min incubation at room temperature. Slides were washed again with PBS and reinserted into the Shadon Sequenza holder (73310017; Thermo Scientific). Slides were then washed twice with PBS containing 0.3% Triton X-100. Anti-BrdU antibody (347580; BD) was diluted 1:50 in PBS–0.3% Triton X-100 and incubated on slides overnight. The next day slides were washed three times with PBS–0.3% Triton X-100, and then secondary anti-mouse antibody–fluorescein (FI-2000; Vector) was added at a dilution of 1:800 in PBS–0.3% Triton X-100. Slides were then incubated in secondary antibody for 1 h in the dark. Slides were washed 3 times in PBS–0.3% Triton X-100 and then counterstained with 4′,6-diamidino-2-phenylindole (DAPI) for 5 min in the dark. Finally, slides were washed twice with PBS–0.3% Triton X-100, twice with PBS, mounted with Slowfade (S36937; Thermo Scientific), and sealed.

TUNEL staining was carried out according to the manufacturer's instructions using an *in situ* cell death detection kit (1168479510; Roche). Briefly, cells were rehydrated with PBS, permeabilized with PBS–0.3% Triton X-100 for 2 min on ice, and then incubated for 1 h with TUNEL reagent. After incubation, slides were washed 3 times with PBS and counterstained with DAPI for 5 min, followed by 2 washes with PBS–0.3% Triton X-100 and 2 washes with PBS. Slides were then mounted with Slowfade (S36937; Thermo Scientific) and sealed.

Images were acquired using a Zeiss Axioskop 40 microscope and Spot flex camera and quantified using velocity image analysis software (PerkinElmer).

CDK2 kinase activity assays. Nuclear extracts were spun down at 14,000 rpm for 30 min to separate protein from cellular debris. Protein (250 μg) from each sample was precleared for 1 h using Dynabeads rotating at 4°C. Samples were then split in half and incubated for an hour with Dynabeads prebound with either IgG or anti-CDK2 (Millipore). Complexes were then washed twice with IP wash buffer (10 mM Tris, pH 7.5, 200 mM NaCl, 1.5 mM $MgCl_2$, 2 mM EDTA, 0.1% NP-40) and twice with kinase buffer (50 mM Tris, pH 7.5, 10 mM $MgCl_2$, 1 mM dithiothreitol [DTT]) and then resuspended in 49 μl of kinase buffer containing 4 μg of recombinant histone H1 (Santa Cruz). ^{32}P-radiolabeled ATP (10 μCi) was incubated with immunoprecipitates for 20 min at 30°C, followed by boiling in SDS-PAGE buffer to stop the reaction. Samples were then run out on a 15% gel, stained with Coomassie to check for loading, and dried and exposed to a phosphosensitive plate to determine ^{32}P incorporation.

ACKNOWLEDGMENTS

We thank Ashley Watson and Nathalie Bérubé for their technical expertise for pituitary sectioning and staining, as well as Charles Ishak, Gabe DiMattia, and Joe Mymryk for frequent discussions and experimental advice.

M.J.T. was funded by OGS, and M.J.T. and M.J.C. were members of the CIHR Strategic Training Program in Cancer Research (CaRTT). M.J.C. was a recipient of a CIHR MD/Ph.D. studentship. F.A.D. is the Wolfe Senior Fellow in Tumor Suppressor Genes. This work was funded by an operating grant from the CIHR (MOP-89765) to F.A.D.

REFERENCES

1. Hanahan D, Weinberg RA. 2011. Hallmarks of cancer: the next generation. Cell 144:646–674. https://doi.org/10.1016/j.cell.2011.02.013.
2. Coller HA. 2007. What's taking so long? S-phase entry from quiescence versus proliferation. Nat Rev Mol Cell Biol 8:667–670.
3. Dick FA, Rubin SM. 2013. Molecular mechanisms underlying RB protein function. Nat Rev Mol Cell Biol 14:297–306. https://doi.org/10.1038/nrm3567.
4. Bertoli C, Skotheim JM, de Bruin RA. 2013. Control of cell cycle transcription during G1 and S phases. Nat Rev Mol Cell Biol 14:518–528. https://doi.org/10.1038/nrm3629.
5. Deshpande A, Sicinski P, Hinds PW. 2005. Cyclins and cdks in development and cancer: a perspective. Oncogene 24:2909–2915. https://doi.org/10.1038/sj.onc.1208618.
6. Hydbring P, Malumbres M, Sicinski P. 2016. Non-canonical functions of cell cycle cyclins and cyclin-dependent kinases. Nat Rev Mol Cell Biol 17:280–292. https://doi.org/10.1038/nrm.2016.27.
7. Sherr CJ, McCormick F. 2002. The RB and p53 pathways in cancer. Cancer Cell 2:103–112. https://doi.org/10.1016/S1535-6108(02)00102-2.
8. Vervoorts J, Luscher B. 2008. Post-translational regulation of the tumor suppressor p27(KIP1). Cell Mol Life Sci 65:3255–3264. https://doi.org/10.1007/s00018-008-8296-7.
9. Besson A, Gurian-West M, Chen X, Kelly-Spratt KS, Kemp CJ, Roberts JM. 2006. A pathway in quiescent cells that controls p27Kip1 stability, subcellular localization, and tumor suppression. Genes Dev 20:47–64. https://doi.org/10.1101/gad.1384406.
10. Malek NP, Sundberg H, McGrew S, Nakayama K, Kyriakides TR, Roberts JM. 2001. A mouse knock-in model exposes sequential proteolytic pathways that regulate p27Kip1 in G1 and S phase. Nature 413:323–327. https://doi.org/10.1038/35095083.
11. Coats S, Flanagan WM, Nourse J, Roberts JM. 1996. Requirement of p27Kip1 for restriction point control of the fibroblast cell cycle. Science 272:877–880. https://doi.org/10.1126/science.272.5263.877.
12. Georgia S, Bhushan A. 2006. p27 regulates the transition of beta-cells from quiescence to proliferation. Diabetes 55:2950–2956. https://doi.org/10.2337/db06-0249.
13. Kossatz U, Dietrich N, Zender L, Buer J, Manns MP, Malek NP. 2004. Skp2-dependent degradation of p27kip1 is essential for cell cycle progression. Genes Dev 18:2602–2607. https://doi.org/10.1101/gad.321004.
14. Sutterluty H, Chatelain E, Marti A, Wirbelauer C, Senften M, Muller U, Krek W. 1999. p45SKP2 promotes p27Kip1 degradation and induces S phase in quiescent cells. Nat Cell Biol 1:207–214. https://doi.org/10.1038/12027.
15. Viatour P, Somervaille TC, Venkatasubrahmanyam S, Kogan S, McLaughlin ME, Weissman IL, Butte AJ, Passegue E, Sage J. 2008. Hematopoietic stem cell quiescence is maintained by compound contributions of the retinoblastoma gene family. Cell Stem Cell 3:416–428. https://doi.org/10.1016/j.stem.2008.07.009.
16. Mason-Richie NA, Mistry MJ, Gettler CA, Elayyadi A, Wikenheiser-Brokamp KA. 2008. Retinoblastoma function is essential for establishing lung epithelial quiescence after injury. Cancer Res 68:4068–4076. https://doi.org/10.1158/0008-5472.CAN-07-5667.
17. Mayhew CN, Bosco EE, Fox SR, Okaya T, Tarapore P, Schwemberger SJ, Babcock GF, Lentsch AB, Fukasawa K, Knudsen ES. 2005. Liver-specific pRB loss results in ectopic cell cycle entry and aberrant ploidy. Cancer Res 65:4568–4577. https://doi.org/10.1158/0008-5472.CAN-04-4221.
18. Dyson N. 1998. The regulation of E2F by pRB-family proteins. Genes Dev 12:2245–2262. https://doi.org/10.1101/gad.12.15.2245.
19. Qin XQ, Chittenden T, Livingston DM, Kaelin WG, Jr. 1992. Identification of a growth suppression domain within the retinoblastoma gene product. Genes Dev 6:953–964. https://doi.org/10.1101/gad.6.6.953.
20. Hiebert SW, Chellappan SP, Horowitz JM, Nevins JR. 1992. The interaction of RB with E2F coincides with an inhibition of the transcriptional activity of E2F. Genes Dev 6:177–185. https://doi.org/10.1101/gad.6.2.177.
21. Qin X-Q, Livingston DM, Ewen M, Sellers WR, Arany Z, Kaelin WG. 1995. The transcription factor E2F-1 is a downstream target of RB action. Mol Cell Biol 15:742–755. https://doi.org/10.1128/MCB.15.2.742.
22. Otterson GA, Chen W, Coxon AB, Khleif SN, Kaye FJ. 1997. Incomplete penetrance of familial retinoblastoma linked to germ-line mutations that result in partial loss of RB function. Proc Natl Acad Sci U S A 94:12036–12040. https://doi.org/10.1073/pnas.94.22.12036.
23. Sellers WR, Novitch BG, Miyake S, Heith A, Otterson GA, Kaye FJ, Lassar AB, Kaelin WG, Jr. 1998. Stable binding to E2F is not required for the retinoblastoma protein to activate transcription, promote differentiation, and suppress tumor cell growth. Genes Dev 12:95–106. https://doi.org/10.1101/gad.12.1.95.
24. Whitaker LL, Su H, Baskaran R, Knudsen ES, Wang JY. 1998. Growth suppression by an E2F-binding-defective retinoblastoma protein (RB): contribution from the RB C pocket. Mol Cell Biol 18:4032–4042. https://doi.org/10.1128/MCB.18.7.4032.
25. Binne UK, Classon MK, Dick FA, Wei W, Rape M, Kaelin WG, Jr, Naar AM, Dyson NJ. 2007. Retinoblastoma protein and anaphase-promoting complex physically interact and functionally cooperate during cell-cycle exit. Nat Cell Biol 9:225–232. https://doi.org/10.1038/ncb1532.
26. Ji P, Jiang H, Rekhtman K, Bloom J, Ichetovkin M, Pagano M, Zhu L. 2004. An Rb-Skp2-p27 pathway mediates acute cell cycle inhibition by Rb and is retained in a partial-penetrance Rb mutant. Mol Cell 16:47–58. https://doi.org/10.1016/j.molcel.2004.09.029.
27. Alexander K, Hinds PW. 2001. Requirement for p27(KIP1) in retinoblastoma protein-mediated senescence. Mol Cell Biol 21:3616–3631. https://doi.org/10.1128/MCB.21.11.3616-3631.2001.
28. Wang H, Bauzon F, Ji P, Xu X, Sun D, Locker J, Sellers RS, Nakayama K, Nakayama KI, Cobrinik D, Zhu L. 2010. Skp2 is required for survival of aberrantly proliferating Rb1-deficient cells and for tumorigenesis in Rb1+/− mice. Nat Genet 42:83–88. https://doi.org/10.1038/ng.498.
29. Zhao H, Bauzon F, Fu H, Lu Z, Cui J, Nakayama K, Nakayama KI, Locker J, Zhu L. 2013. Skp2 deletion unmasks a p27 safeguard that blocks

tumorigenesis in the absence of pRb and p53 tumor suppressors. Cancer Cell 24:645–659. https://doi.org/10.1016/j.ccr.2013.09.021.
30. Cecchini MJ, Thwaites M, Talluri S, Macdonald JI, Passos DT, Chong JL, Cantalupo P, Stafford P, Saenz-Robles MT, Francis SM, Pipas JM, Leone G, Welch I, Dick FA. 2014. A retinoblastoma allele that is mutated at its common E2F interaction site inhibits cell proliferation in gene targeted mice. Mol Cell Biol 34:2029–2045. https://doi.org/10.1128/MCB.01589-13.
31. Park MS, Rosai J, Nguyen HT, Capodieci P, Cordon-Cardo C, Koff A. 1999. p27 and Rb are on overlapping pathways suppressing tumorigenesis in mice. Proc Natl Acad Sci U S A 96:6382–6387. https://doi.org/10.1073/pnas.96.11.6382.
32. Buttitta LA, Edgar BA. 2007. Mechanisms controlling cell cycle exit upon terminal differentiation. Curr Opin Cell Biol 19:697–704. https://doi.org/10.1016/j.ceb.2007.10.004.
33. Busuttil RA, Rubio M, Dolle ME, Campisi J, Vijg J. 2003. Oxygen accelerates the accumulation of mutations during the senescence and immortalization of murine cells in culture. Aging Cell 2:287–294. https://doi.org/10.1046/j.1474-9728.2003.00066.x.
34. Williams BO, Remington L, Albert DM, Mukai S, Bronson RT, Jacks T. 1994. Cooperative tumorigenic effects of germline mutations in Rb and p53. Nat Genet 7:480–484. https://doi.org/10.1038/ng0894-480.
35. Harrison DJ, Hooper ML, Armstrong JF, Clarke AR. 1995. Effects of heterozygosity for the Rb-1t19neo allele in the mouse. Oncogene 10:1615–1620.
36. Bilodeau S, Roussel-Gervais A, Drouin J. 2009. Distinct developmental roles of cell cycle inhibitors p57Kip2 and p27Kip1 distinguish pituitary progenitor cell cycle exit from cell cycle reentry of differentiated cells. Mol Cell Biol 29:1895–1908. https://doi.org/10.1128/MCB.01885-08.
37. Cobrinik D. 2005. Pocket proteins and cell cycle control. Oncogene 24:2796–2809. https://doi.org/10.1038/sj.onc.1208619.
38. Morris EJ, Dyson NJ. 2001. Retinoblastoma protein partners. Adv Cancer Res 82:1–54. https://doi.org/10.1016/S0065-230X(01)82001-7.
39. Finn RS, Dering J, Conklin D, Kalous O, Cohen DJ, Desai AJ, Ginther C, Atefi M, Chen I, Fowst C, Los G, Slamon DJ. 2009. PD 0332991, a selective cyclin D kinase 4/6 inhibitor, preferentially inhibits proliferation of luminal estrogen receptor-positive human breast cancer cell lines in vitro. Breast Cancer Res 11:R77. https://doi.org/10.1186/bcr2419.
40. Rader J, Russell MR, Hart LS, Nakazawa MS, Belcastro LT, Martinez D, Li Y, Carpenter EL, Attiyeh EF, Diskin SJ, Kim S, Parasuraman S, Caponigro G, Schnepp RW, Wood AC, Pawel B, Cole KA, Maris JM. 2013. Dual CDK4/CDK6 inhibition induces cell-cycle arrest and senescence in neuroblastoma. Clin Cancer Res 19:6173–6182. https://doi.org/10.1158/1078-0432.CCR-13-1675.
41. Gelbert LM, Cai S, Lin X, Sanchez-Martinez C, Del Prado M, Lallena MJ, Torres R, Ajamie RT, Wishart GN, Flack RS, Neubauer BL, Young J, Chan EM, Iversen P, Cronier D, Kreklau E, de Dios A. 2014. Preclinical characterization of the CDK4/6 inhibitor LY2835219: in-vivo cell cycle-dependent/independent anti-tumor activities alone/in combination with gemcitabine. Investig New Drugs 32:825–837. https://doi.org/10.1007/s10637-014-0120-7.
42. Cadoo KA, Gucalp A, Traina TA. 2014. Palbociclib: an evidence-based review of its potential in the treatment of breast cancer. Breast Cancer (Dove Med Press) 6:123–133.
43. Cecchini MJ, Amiri M, Dick FA. 2012. Analysis of cell cycle position in mammalian cells. J Vis Exp 59:e3491.
44. Thwaites MJ, Cecchini MJ, Dick FA. 2014. Analyzing RB and E2F during the G1-S transition. Methods Mol Biol 1170:449–461. https://doi.org/10.1007/978-1-4939-0888-2_24.
45. Fero ML, Rivkin M, Tasch M, Porter P, Carow CE, Firpo E, Polyak K, Tsai LH, Broudy V, Perlmutter RM, Kaushansky K, Roberts JM. 1996. A syndrome of multiorgan hyperplasia with features of gigantism, tumorigenesis, and female sterility in p27(Kip1)-deficient mice. Cell 85:733–744. https://doi.org/10.1016/S0092-8674(00)81239-8.
46. Ritchie K, Watson LA, Davidson B, Jiang Y, Berube NG. 2014. ATRX is required for maintenance of the neuroprogenitor cell pool in the embryonic mouse brain. Biol Open 3:1158–1163. https://doi.org/10.1242/bio.20148730.